ICIC Express Letters
Part B: Applications
Volume **7**, Number **7**, July **2016**

ICIC International ©2016 ISSN 2185-2766
pp. **1551–1558**

ESO-BASED COMMAND-FILTERED BACKSTEPPING CONTROL FOR VARIABLE SPEED WIND TURBINES

Wenxu Yan[1], Dezhi Xu[1], Peisi Ji[2] and Nan Ji[1]

[1]School of Internet of Things Engineering
Jiangnan University
No. 1800, Lihu Avenue, Wuxi 214122, P. R. China
lutxdz@126.com

[2]Haian Power Supply Company
Nantong 226681, P. R. China

Received December 2015; accepted March 2016

Abstract. *In this paper, an extend state observer (ESO)-based command-filtered backstepping control strategy is proposed for a variable speed wind turbine (VSWT) using VSWT's input and output measurements. First, the dynamic model of VSWT is described. Next, a model transformation is proposed for VSWT that we convert the VSWT system into a strict-feedback form through state transformation. Then, an ESO is given to estimate the unknown dynamic model. Next, the command-filtered backstepping controller is proposed for the VSWT system. Finally, simulation results are given to demonstrate the effectiveness and potential of the proposed constrained control scheme.*
Keywords: Extend state observer, Control saturation, Command-filtered backstepping, Variable speed wind turbine

1. **Introduction.** Wind is a kind of renewable energy with great potential. On the earth there are about 10 billion kilowatts wind resources used to produce electricity, which is almost 10 times more than the present amount of hydroelectric power [1-4]. With the development of control theory, the wind power generator control system improves from the initial fixed pitch and constant speed control to the current variable pitch and variable speed control. Due to the great advantages of VSWT in the utilization of wind energy, the VSWT has become the main control study object [5-10]. Because of the factors of the inherent nonlinearity and uncertainty in VSWT system, people have tried to use various nonlinear control theories based on models on the control of VSWT systems in recent years [8-11].

Backstepping is a method based on recursive Lyapunov for nonlinear dynamical systems [12]. It breaks the whole system into several lower order systems which can deal with the complex system with useful nonlinearities easily, so it has wider application range than output feedback [13-16]. Due to the recursive structure, some state variables called virtual controls and intermediate control laws are designed for the recursive controller.

Inspired by the work of technique [12,15,16], we give an ESO-based command-filtered backstepping control approach for VSWT in this paper. It is a constrained control strategy after the model transformation of VSWT. The major advantages of this dissertation are displayed as follows. In the design procedure of controller: 1) only the output measurement of VSWT is required; 2) explicit model dynamics and structural information of the VSWT do not need to be known; 3) the proposed control strategy can reduce the impact of derivative signal and control saturation.

The rest of this paper is organized as follows. A brief description of VSWT is in Section 2. In Section 3, main results of ESO-based command-filtered backstepping control are

proposed. Simulation results are presented to show the effectiveness of the proposed technique in Section 4. Finally, some conclusions are made at end of this paper.

2. **System Model and Problem Formulation.** The basic composition of VSWT includes three parts which are wind turbines, growth container and generator. The block diagram of VSWT is shown in Figure 1.

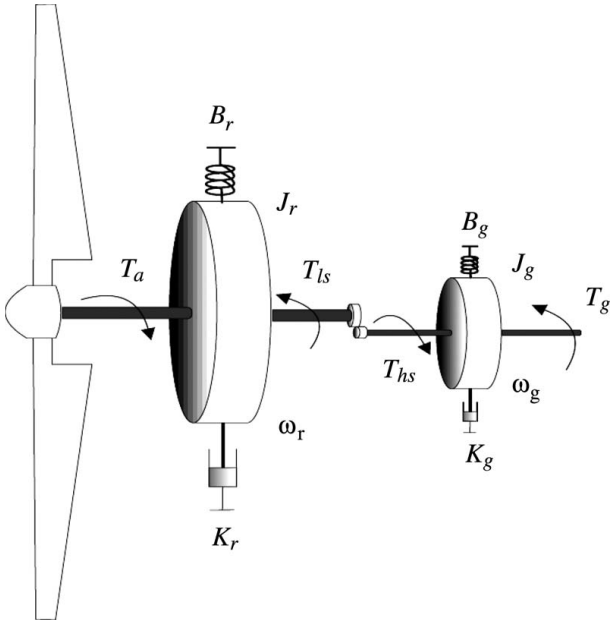

FIGURE 1. Schematic block diagram for the structure of VSWT [8]

The rotor dynamic is described as

$$J_r\dot{\omega}_r = T_a - K_r\omega_r - B_r\int_0^t \omega_r(\tau)\mathrm{d}\tau - T_{ls} \tag{1}$$

where J_r, T_a, K_r, ω_r, B_r, and T_{ls} denote rotor inertia, aerodynamic torque, rotor external damping, rotor speed, rotor external stiffness and low-speed torque, respectively. The generator dynamic is given as

$$J_g\dot{\omega}_g = T_{hs} - K_g\omega_g - B_g\int_0^t \omega_g(\tau)\mathrm{d}\tau - T_g \tag{2}$$

where J_g, ω_g, T_{hs}, K_g, B_g and T_g represent generator inertia, generator speed, high-speed torque, generator external damping, generator external stiffness and generator electromagnetic torque, respectively. Because of the gearbox ratio, the following relationship (3) is obtained for the speed ω_r, ω_g, and torque T_{ls}, T_{hs}.

$$n_g = \frac{\omega_g}{\omega_r} = \frac{T_{ls}}{T_{hs}} \tag{3}$$

According to Equation (1) to Equation (3), since $J_t \neq 0$, we can obtain

$$\dot{\omega}_r = \frac{1}{J_t}\left(T_a - K_t\omega_r - B_t\int_0^t \omega_r(\tau)\mathrm{d}\tau - T_g\right) \tag{4}$$

where turbine total inertia J_t, turbine total external damping K_t, turbine total external stiffness B_t and generator electromagnetic torque T_g are respectively defined as

$$J_t = J_r + n_g^2 J_g,\ K_t = K_r + n_g^2 K_g,\ B_t = B_r + n_g^2 B_g,\ T_g = n_g T_{em}$$

Therein, T_a and T_{em} can be described as follows [6,9],

$$T_a = K_w \cdot \omega_r^2,\ T_{em} = K_\phi \cdot c(I_f) \tag{5}$$

where K_w is the wind speed to power transfer parameter depending on factors like air density, radius of the rotor, the wind speed and the pitch angle. $c(I_f)$ is the flux in the generating system function. The electrical subsystem dynamic of VSWT is governed by [9]

$$\dot{I}_f = -\frac{R_f}{L} I_f + \frac{1}{L} u_f \tag{6}$$

where I_f, u_f, R_f and L denote field current, field voltage, resistance of the rotor field and constant inductance of the circuit, respectively. Hence, from Equation (4) to Equation (6), the dynamic model of VSWT can be described as

$$\begin{cases} \dot{\omega}_r = \underbrace{\dfrac{K_w}{J_t}\omega_r^2 - \dfrac{K_t}{J_t}\omega_r - \dfrac{B_t}{J_t}\displaystyle\int_0^t \omega_r(\tau)\mathrm{d}\tau - \dfrac{n_g K_\phi}{J_t} c(I_f)}_{f_1(\omega_r, \theta_r, I_f)} \\ \dot{I}_f = -\dfrac{R_f}{L} I_f + \dfrac{1}{L} u_f \end{cases} \tag{7}$$

where angle $\theta_r = \int_0^t \omega_r(\tau)\mathrm{d}\tau$ and K_ϕ denote machine-related constant. Assume that function $f_1(\omega_r, \theta_r, I_f)$, R_f and L are all unknown. The control objective of this paper is to ensure that output rotor speed ω_r can follow a reference trajectory ω_d. The controller design and the stability analysis also require the desired reference trajectory to be first order integrable, that is

$$\int_0^T |\omega_d(\tau)|\,\mathrm{d}\tau < \infty$$

with T being finite (i.e., $\omega_d \in \mathcal{L}_1 \cap \mathcal{L}_\infty$ and $\dot{\omega}_d, \ddot{\omega}_d \in \mathcal{L}_\infty$).

3. Main Results.

3.1. Model transformation.

Define new state $x_1 = \omega_r$, $x_2 = \dot{x}_1 = \dot{\omega}_r = f_1(\omega_r, \theta_r, I_f)$. Then the time derivative of x_2 can be expressed as

$$\begin{aligned} \dot{x}_2 &= \dot{f}_1(\omega_r, \theta_r, I_f) \\ &= \frac{\partial f_1(\omega_r, \theta_r, I_f)}{\partial \omega_r}\dot{\omega}_r + \frac{\partial f_1(\omega_r, \theta_r, I_f)}{\partial \theta_r}\omega_r + \frac{\partial f_1(\omega_r, \theta_r, I_f)}{\partial I_f}\dot{I}_f \\ &= f(\bar{x}) + g(\bar{x})u_f \end{aligned} \tag{8}$$

where

$$\begin{aligned} f(\bar{x}) = f(\omega_r, \theta_r, I_f) = &\frac{\partial f_1(\omega_r, \theta_r, I_f)}{\partial \omega_r} f_1(\omega_r, \theta_r, I_f) \\ &+ \frac{\partial f_1(\omega_r, \theta_r, I_f)}{\partial \theta_r}\omega_r - \frac{R_f \cdot I_f \cdot \partial f_1(\omega_r, \theta_r, I_f)}{L \cdot \partial I_f} \end{aligned}$$

and

$$g(\bar{x}) = g(\omega_r, \theta_r, I_f) = \frac{\partial f_1(\omega_r, \theta_r, I_f)}{L \cdot \partial I_f}$$

with $\bar{x} = [\omega_r, \theta_r, I_f]^T$. Hence, the dynamic model of VSWT (7) is now transformed as

$$\begin{cases} \dot{x}_1 = x_2 \\ \dot{x}_2 = f(\bar{x}) + g(\bar{x})u_f \\ y = x_1 \end{cases} \tag{9}$$

To account for the uncertainties in VSWT parameters, we rewrite the dynamics (9) as

$$\begin{cases} \dot{x}_1 = x_2 \\ \dot{x}_2 = d(t) + g_o u_f \\ y = x_1 \end{cases} \tag{10}$$

where g_o is the best available estimation of $g(\bar{x})$, while Δg is associated uncertainties. The variable $d(t) = f(\bar{x}) + \Delta g u_f$ is the combined uncertainty and may also include other sources such as external disturbance in the system.

3.2. **Extend state observer design.** We assume that only power angle ($\omega_r = y$) can be measured in (7). So in this paper, the third-order ESO is designed, which is used to estimate the state x_2 and combined uncertainty $d(t)$. Define the combined uncertainty $d(t)$ as an extended state x_3. Let $x_3 = d(t)$, $\dot{x}_3 = \varpi$, where ϖ is an unknown function. We assume that $|\varpi(t)| < r$. Then system (10) is equivalent to

$$\begin{cases} \dot{x}_1 = x_2 \\ \dot{x}_2 = x_3 + g_o u_f \\ \dot{x}_3 = \varpi \\ y = x_1 \end{cases} \tag{11}$$

In order to estimate the state x_2 and the combined uncertainty $d(t)$, we design the following third-order ESO [12,14]:

$$\begin{cases} \dot{\hat{x}}_1 = \hat{x}_2 - l_1 \tilde{y} \\ \dot{\hat{x}}_2 = \hat{x}_3 + g_o u_f - l_2 \text{fal}(\tilde{y}, \alpha_1, \sigma_1) \\ \dot{\hat{x}}_3 = -l_3 \text{fal}(\tilde{y}, \alpha_2, \sigma_2) \\ \hat{y} = \hat{x}_1 \end{cases} \tag{12}$$

where $\tilde{y} = y - \hat{y} = x_1 - \hat{x}_1$ and $\hat{x}_1, \hat{x}_2, \hat{x}_3$ are the observers of x_1, x_2, x_3. $0 < \alpha_1 < 1$, $0 < \alpha_2 < 1$, $\sigma_1 > 0$, $\sigma_2 > 0$, $l_i > 0$, $i = 1, 2, 3$ are parameters of observer (12). And the nonlinear function fal$(\cdot)$ is defined as

$$\text{fal}(\epsilon, \alpha, \sigma) = \begin{cases} |\gamma|^{\alpha} \text{sgn}(\gamma), & |\gamma| > \sigma \\ \dfrac{\gamma}{\sigma^{1-\alpha}}, & |\gamma| \le \sigma \end{cases} \tag{13}$$

Letting T be sampling period of control, in general, σ is selected as $\sigma = 5 \sim 10T$. Until now, there is no reliable theoretical analysis method available for third-order ESO. Fortunately, according to [12], if suitable parameters of observer (12) are selected, the following results can be obtained.

$$\begin{aligned} &\lim_{t \to \infty} |\tilde{x}_2| < l_1 \left(\frac{r}{l_3} \right)^{1/\alpha_2} = \varepsilon_{x_2} \\ &\lim_{t \to \infty} |\tilde{d}| = \lim_{t \to \infty} |\tilde{x}_3| < l_2 \left(\frac{r}{l_3} \right)^{1/\alpha_2} = \varepsilon_d \end{aligned} \tag{14}$$

where $\tilde{x}_2 = x_2 - \hat{x}_2$, $\tilde{d} = d - \hat{d}$ and $\tilde{x}_3 = x_3 - \hat{x}_3$. Hence, we know the suitable observer parameters can make the state estimation errors $\tilde{x}_1$, $\tilde{x}_2$ and combined uncertainty error $\tilde{d} = \tilde{x}_3$ uniformly ultimately bounded (UUB).

Equation (15) denotes the uniform form of observers (12):

$$\begin{cases} \dot{\hat{x}}_1 = \hat{x}_2 + \kappa_1 \\ \dot{\hat{x}}_2 = \text{b}u + \kappa_2 \end{cases} \tag{15}$$

where $\kappa_1 = -l_1 \tilde{y}$, $\kappa_2 = \hat{x}_3 - l_2 \text{fal}(\tilde{y}, \alpha_1, \sigma_1)$ and $\text{b} = g_o$.

3.3. **Command-filtered backstepping controller design.** According to above results, Equation (15) is a strict-feedback form obviously, so the backstepping control can be adopted for a controller of VSWT. The traditional backstepping control has an obvious disadvantage that it can be easily affected by differential expansion and control saturation problems. Some researchers have proposed a constrained command filter into the adaptive backstepping control system to solve this problem [15,16]. Command filter can eliminate the negative impact of the control saturation and derivative signal. The traditional backstepping control and command-filtered backstepping control are very different in design idea and design process. The structure of the ESO-based command-filtered backstepping control algorithm is depicted as Figure 2.

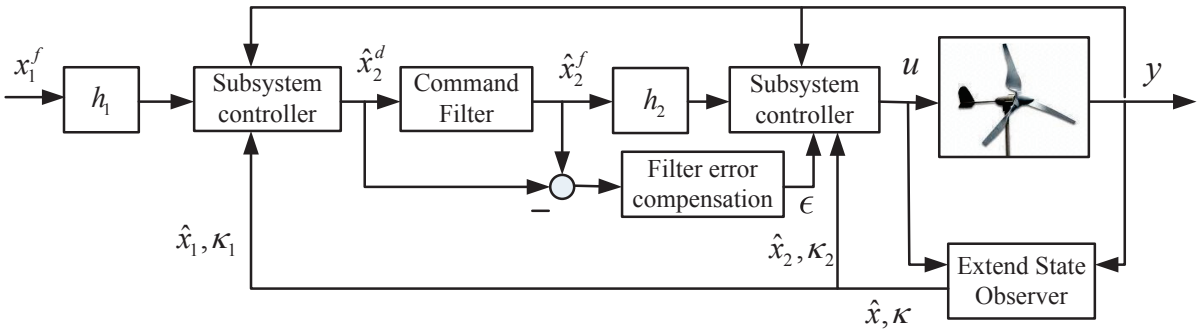

FIGURE 2. Structure of the proposed ESO-based command-filtered backstepping control for VSWT system

Define the tracking error e_1 and e_2. The functions of e_1 and e_2 are written as

$$e_1 = \hat{x}_1 - x_1^f, \quad e_2 = \hat{x}_2 - \hat{x}_2^f \tag{16}$$

where x_1^f and $\hat{x}_2^f$ are the filtered-command of x_1^d and $\hat{x}_2$, respectively. Therein, $x_1^d = \omega_d$, and ω_d is a reference trajectory. According to Equation (15) and Equation (16), $\dot{e}_1$ and $\dot{e}_2$ can be obtained that

$$\dot{e}_1 = \hat{x}_2 + \kappa_1 - \dot{x}_1^f \tag{17}$$

$$\dot{e}_2 = \mathrm{b}u + \kappa_2 - \dot{\hat{x}}_2^f \tag{18}$$

The first Lyapunov function is defined as follows

$$V_1 = \frac{1}{2} e_1^2$$

The time derivative of V_1 is described as

$$\dot{V}_1 = e_1 \left(\hat{x}_2 + \kappa_1 - \dot{x}_1^f \right) \tag{19}$$

The virtual controller of the outer-loop can be defined as

$$\hat{x}_2^d = \dot{x}_1^f - \kappa_1 - h_1 e_1 \tag{20}$$

where h_1 is a preset positive definite constant. From Equation (19) and Equation (20), we achieve the result that $\dot{V}_1 \leq 0$. Then, let $\hat{x}_2^d$ through a filter [15,16], the structure of the command filter is shown in Figure 3, and the dynamic model of constrained command filter is defined as

$$\begin{Bmatrix} \dot{\mathrm{q}}_1 \\ \dot{\mathrm{q}}_2 \end{Bmatrix} = \begin{bmatrix} \mathrm{q}_2 \\ 2\varphi\iota_n \left[S_R \left(\frac{\iota_n^2}{2\varphi\iota_n} \left(S_M \left(u \right) - \mathrm{q}_1 \right) \right) - \mathrm{q}_2 \right] \end{bmatrix} \tag{21}$$

where

$$\begin{bmatrix} \mathrm{q}_1 \\ \mathrm{q}_2 \end{bmatrix} = \begin{bmatrix} x^f \\ \dot{x}^f \end{bmatrix} \text{ and } u = x^d$$

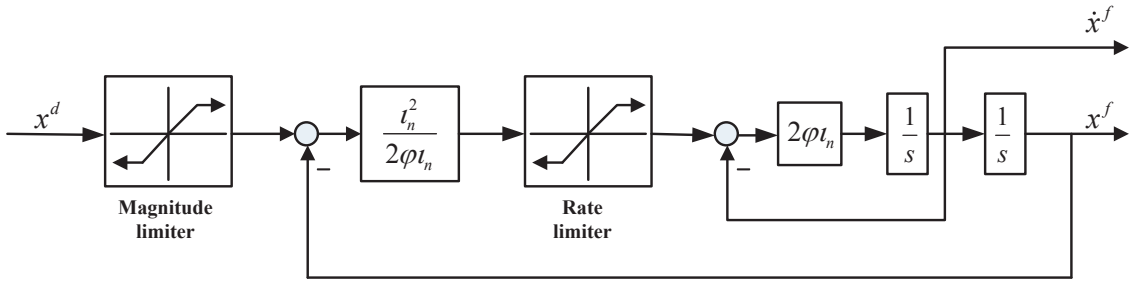

FIGURE 3. Structure of constrained command filters

Therein, φ, ι_n and x^f denote the damping, the bandwidth of filter and the output of the constrained command filter, respectively.

We define a new tracking error $\bar{e}_1 = e_1 - \epsilon$, where ϵ represents the filter error compensation that can be written as

$$\dot{\epsilon} = -h_1\epsilon + \hat{x}_2^f - \hat{x}_2^d \tag{22}$$

We define an another Lyapunov function

$$V_2 = \frac{1}{2}\bar{e}_1^2 + \frac{1}{2}e_2^2$$

Then, the time derivative of V_2 is described as the following

$$\begin{aligned}\dot{V}_2 &= \bar{e}_1\dot{\bar{e}}_1 + e_2\dot{e}_2 \\ &= \bar{e}_1\left(\hat{x}_2 + \kappa_1 - \dot{x}_1^f + h_1\epsilon - \hat{x}_2^f + \hat{x}_2^d\right) + e_2\left(\mathrm{b}u + \kappa_2 - \dot{\hat{x}}_2^f\right) \\ &= -\bar{e}_1\left(h_1\bar{e}_1 + \hat{x}_2^f - \hat{x}_2\right) + e_2\left(\mathrm{b}u + \kappa_2 - \dot{\hat{x}}_2^f\right) \\ &= -h_1\bar{e}_1^2 + \bar{e}_1e_2 + e_2\left(\mathrm{b}u + \kappa_2 - \dot{\hat{x}}_2^f\right)\end{aligned}$$

When the global control law is selected as

$$u = \mathrm{b}^{-1}\left(-h_2e_2 - \kappa_2 - \bar{e}_1 + \dot{\hat{x}}_2^f\right) \tag{23}$$

We can get the result that the function $\dot{V}_2$ is rewritten as

$$\dot{V}_2 = -h_1\bar{e}_1^2 - h_2e_2^2 \le 0 \tag{24}$$

where h_2 is also a preset positive definite constant. From Equation (24), we have the information that $\bar{e}_1$, e_2 are uniformly ultimately bounded. Moreover, we can obtain the conclusion that the whole system is uniformly ultimately bounded combined with the previous results in this paper.

4. **Simulation Results.** In this section, the simulation is shown to demonstrate the validity of the proposed ESO-based command-filtered backstepping control algorithm. In simulation, the system parameters of VSWT are chosen as same as [6,9], which are considered as $R_f = 0.02\Omega$, $L = 0.001H$, $J_t = 24490$, $B_t = 52$, $K_t = 52$, $K_\omega = 3$, $n_g = 30$, $K_\phi = 1.7$, $c(I_f) = 1000I_f$.

And the reference angular velocity signal $\omega_d(t)$ is selected by the following case, which is

$$\omega_d(t) = 2 + \sin(0.5t)$$

For the simulation, we choose ESO parameters as $l_1 = 10^2$, $l_2 = 10^4$, $l_3 = 10^5$, $\alpha_1 = \alpha_2 = 0.9$, $\sigma_1 = 10^2$, and $\sigma_2 = 10^3$. The controller gains are selected as $g_0 = -2000$, and $h_1 = h_2 = 5000$. The initial state values are $\omega_r(0) = 1$, and $I_f(0) = 0$.

The results of simulation are shown in Figures 4 and 5, where Figure 4 illustrates the reference ω_d, actual rotor velocity ω_r, the field voltage u_f (control input). Figure

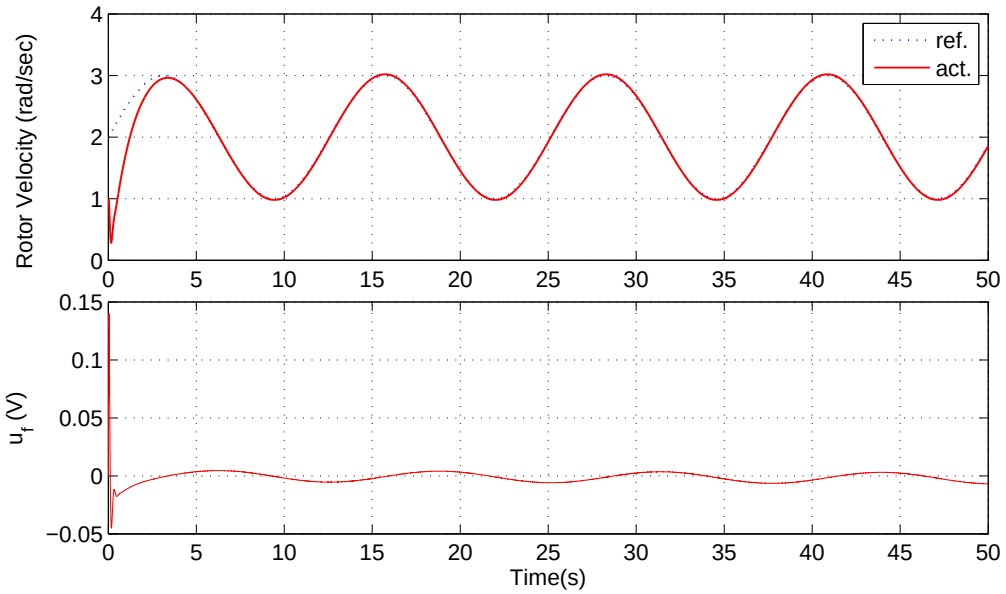

FIGURE 4. The VSWT output and control input responses curve

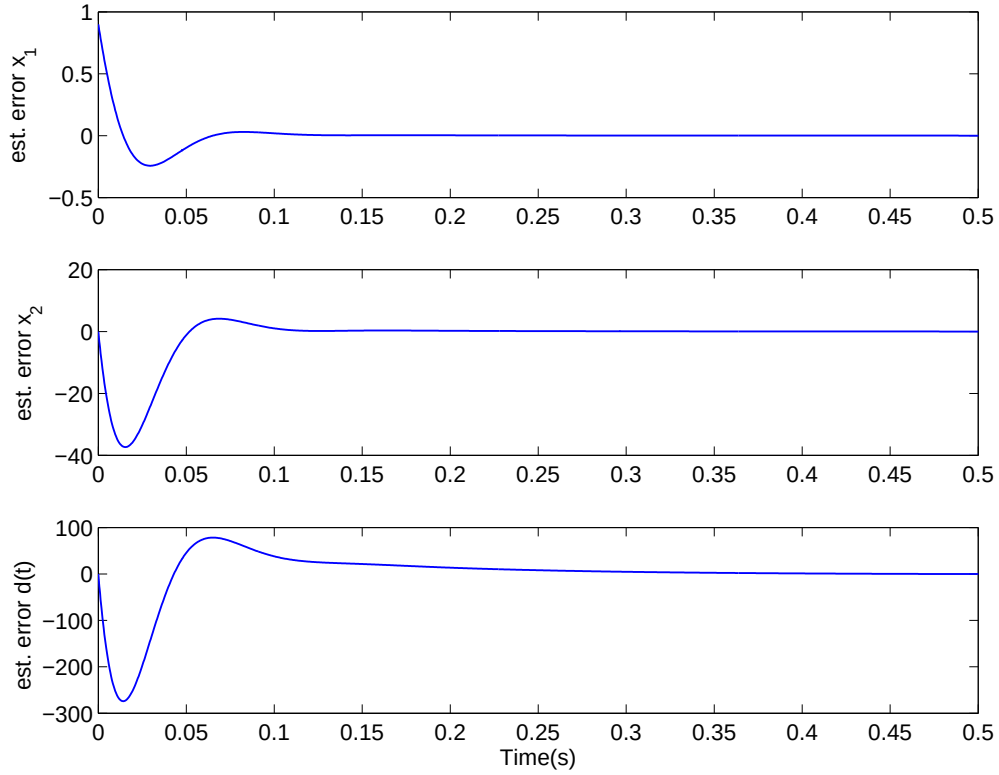

FIGURE 5. The states estimation errors by ESO

5 shows the estimation errors for x_1, x_2 and $d(t)$. It can be seen from the response figures, tracking and estimation errors converge to very small values, and further more the ESO-based command-filtered backstepping controller achieves good performance.

5. **Conclusion.** In this paper, we have developed an ESO-based command-filtered backstepping control strategy, which provides an alternative to the VSWT control problem.

A model transformation is proposed for VSWT dynamic model that converts the VSWT system into a strict-feedback form through state transformation. This proposed control approach of VSWT is particularly effective while the explicit analytical model of VSWT is difficult to develop and the states are not fully measurable. Our focus of this paper is on the uncertainty, and the incomplete measurable states. The simulation results have validated the proposed nonlinear control algorithm.

Acknowledgment. This work is supported by the National Natural Science Foundation of China (61503156, 51405198), the Fundamental Research Funds for the Central Universities (JUSRP11562, NJ20150011, JUSRP51406A).

REFERENCES

[1] J. F. Manwell, J. McGowan and A. Rogers, *Wind Energy Explained: Theory, Design and Applications*, Wiley, Hoboken, NJ, 2002.

[2] Z. Chen, J. M. Guerrero and F. Blaabjerg, A review of the state of the art of power electronics for wind turbines, *IEEE Trans. Power Electron.*, vol.24, no.8, pp.1859-1875, 2009.

[3] F. D. Bianchi, H. D. Battista and R. J. Mantz, *Wind Turbine Control Systems: Principles, Modelling and Gain Scheduling Design*, 2nd Edition, Springer, 2006.

[4] T. Burton, D. Sharpe, N. Jenkins and E. Bossanyi, *Wind Energy Handbook*, Wiley, Hoboken, NJ, 2001.

[5] O. Barambones, J. M. Durana and M. D. Sen, Robust speed control for a variable speed wind turbine, *International Journal of Innovative Computing, Information and Control*, vol.8, no.11, pp.7627-7640, 2012.

[6] Y. D. Song, B. Dhinarakaran and X. Y. Bao, Variable speed control of wind turbines using nonlinear and adaptive algorithms, *Journal of Wind Engineering and Industrial Aerodynamics*, vol.85, no.3, pp.293-308, 2000.

[7] B. Boukhezzar and H. Siguerdidjane, Nonlinear control of a variable speed wind turbine using a two-mass model, *IEEE Trans. Energy Convers.*, vol.26, no.1, pp.149-162, 2011.

[8] Y. Bao, H. Wang and J. Zhang, Adaptive inverse control of variable speed wind turbine, *Nonlinear Dyn.*, vol.61, no.4, pp.819-827, 2010.

[9] U. Ozbay, E. Zergeroglu and S. Sivrioglu, Adaptive backstepping control of variable speed wind turbines, *Int. J. Control*, vol.81, no.6, pp.910-919, 2008.

[10] B. Beltran, T. Ahmed-Ali and M. E. Benbouzid, High order sliding-mode control of variable-speed wind turbines, *IEEE Trans. Ind. Electron.*, vol.56, no.9, pp.3314-3321, 2009.

[11] S. A. Frost, M. J. Balas and A. D. Wright, Direct adaptive control of a utility-scale wind turbine for speed regulation, *Int. J. Robust Nonlinear Control*, vol.19, no.1, pp.59-71, 2008.

[12] J. Han, From PID to active disturbance rejection control, *IEEE Trans. Ind. Electron.*, vol.56, no.3, pp.900-906, 2009.

[13] Y. Xia, P. Shi, G. P. Liu, D. Rees and J. Han, Active disturbance rejection control for uncertain multivariable systems with time delay, *IET Control Theory Appl.*, vol.1, no.1, pp.75-81, 2007.

[14] Y. Huang, K. Xu, J. Han and J. Lam, Flight control design using extended state observer and non-smooth feedback, *Proc. of the 40th IEEE Conf. Decision Control*, Orlando, FL, pp.223-228, 2001.

[15] B. Jiang, D. Xu, P. Shi and C. Lim, Adaptive neural observer-based backstepping fault tolerant control for near space vehicle under control effector damage, *IET Control Theory Appl.*, vol.8, no.9, pp.658-666, 2014.

[16] D. Xu, B. Jiang, H. Liu and P. Shi, Decentralized asymptotic fault tolerant control of near space vehicle with high order actuator dynamics, *Journal of the Franklin Institute*, vol.350, pp.2519-2534, 2013.